CASE STUDY

LANDSCAPE READING FOR ALPINE RIVERS: A CASE STUDY FROM THE RIVER BIYA

Lisa Schmalfuß[1*], Christoph Hauer[1], Liubov V. Yanygina[2], Martin Schletterer[3]

[1]Institute of Hydraulic Engineering and River Research, University of Natural Resources and Applied Life Sciences, 1180, Vienna, Austria

[2]Institute for Water and Environmental Problems SB RAS, Ulitsa Molodezhnaya 1, 656038, Barnaul, Russia

[3]Institute of Hydrobiology and Aquatic Ecosystem Management, University of Natural Resources and Applied Life Sciences, 1180, Vienna, Austria

***Corresponding author:** lisa.schmalfuss@boku.ac.at

Received: April 11th, 2021 / Accepted: November 11th, 2022 / Published: December 31st, 2022

https://DOI-10.24057/2071-9388-2022-046

ABSTRACT. Anthropogenic stressors have altered the hydromorphological characteristics of rivers worldwide. Environmental guiding principles are essential for planning sustainable river restoration measures. The alpine river Biya, located in the Russian Altai mountains, originates from Lake Teletskoye and joins the Katun near Biysk, forming the Ob. The Biya represents a hydromorphological reference system in anthropogenically 'least-disturbed' condition. The presented study aimed to assess the river's undisturbed morphology in relationship with the geological history of three different river stretches based on an adapted landscape reading approach using remote sensing information (ASTER GDEM v3). The established widths of the active channel, active floodplain and morphological floodplain as well as the longitudinal section were used to explain the differences between upper, middle, and lower Biya. The results confirm differences in the geological origins between the upper Biya, which has previously been described as the least developed and narrowest, and the other two stretches based on the analyses of morphological parameters. Morphological floodplain width could best explain the differences between upper (0-86 km), middle (86-196 km), and lower Biya (196-301 km). The study further showed a clear relationship between the variations in river patterns and adjacent topographic structures (valley confinements, tributary interactions), highlighting that any assessment of river morphology must consider the wider surroundings of a river stretch. The presented morphological observations and analyses of the Biya show that easily obtainable parameters can detect differences in the morphological history of river stretches within the same catchment, supporting process understanding.

KEYWORDS: hydromorphology, glacial history, sinuosity, channel evolution, remote sensing

CITATION: Schmalfuß L., Hauer C., Yanygina L. V., Schletterer M. (2022). Landscape Reading for Alpine Rivers: A Case Study from the river Biya. Geography, Environment, Sustainability, 4(15), 196-213
https://DOI-10.24057/2071-9388-2022-046

ACKNOWLEDGEMENTS: The authors thank Friedrich Seidl for providing the grain size distribution data that was included in the description of the Biya.

Conflict of interests: The authors reported no potential conflict of interest.

INTRODUCTION

Water covers 71% of our planet (USGS 2019) and contributes majorly to the shape and character of the Earth's surface as it travels from source to sea. River (eco-) systems are the setting of critical environmental processes, like sediment or nutrient transport (Newbold et al. 1982) and connect a wide range of different ecosystems and biotic communities (Vannote et al. 1980), acting on a four-dimensional level (Ward 1989). Connectivity throughout whole river systems is necessary for the functioning of all associated processes (Grill et al. 2015). Changing single parameters within a river's catchment can lead to drastic changes in the dynamic equilibrium (Nanson and Huang 2018). Following centuries of anthropogenic interferences, rivers are affected by a multitude of stressors (Lemm et al. 2020). Rivers are among the most heavily degraded ecosystems in the world (Tickner et al. 2020, Malmqvist and Rundle 2002, Sala et al. 2000), putting freshwater megafauna at severe threat (He et al. 2019, Zarfl et al. 2019, He et al. 2018) and reducing the capacity to further fulfil ecosystem services that human societies rely on (Feio et al. 2022, Abily et al. 2021). The natural regimes of most of the world's larger river systems were altered, and it is assumed that 48% of rivers worldwide are moderately to severely impacted by flow regulation, fragmentation, or both (Grill et al. 2015). Next to these direct anthropogenic impacts, less obvious, indirect changes, like climate or land use change, are continuously transforming hydrological boundary conditions, as well as the sediment cycle, leading to significant alterations in water temperatures and other abiotic habitat factors and consequently destabilising

many riverine ecosystems (Liu et al. 2020, Sala et al. 2000). Ecologically intact, or free flowing rivers have become increasingly rare and are largely restricted to remote areas with lower degrees of human development, usually found in snow climates (Feio et al. 2022, Grill et al. 2019).

There is an urgent need for action and growing demand to reorganise river management based on an international and interdisciplinary approach so that the functionality of the exposed ecosystems is improved and not compromised any further (Feio et al. 2021, Muhar 1996). It is essential that river restoration approaches build on a sound understanding of the complex ecosystem processes (Tickner et al. 2020), also taking into account channel evolution (Scorpio et al. 2020). Our understanding of river morphological processes and interactions must be continuously advanced since it provides the foundation to combat current shortcomings in river health.

When trying to understand why a river looks the way it does, the focus must be put on the temporal context and the geological history of the river's catchment area: Fluvial development is subject to changes in climate as well as tectonic processes (Vandenberghe et al. 2018) that also interact with sediment dynamics and resulting changes in channel bed elevation (Anderson and Konrad 2019). Processes associated with (past) glaciation, for example, exert influence on many rivers in the temperate climate zone. These processes are majorly responsible for reshaping the landscape by eroding older sediments and reorganising river pathways and the sedimentary system through the stages of glaciation (Sokołowski et al. 2021, Comiti et al. 2019, Fildani et al. 2018). Glacial-interglacial cycles are major drivers of river incision and aggradation (Huang et al. 2019 Malatesta and Avouac 2018). Glacial and periglacial erosion provide vast amounts of sediment (Huang et al. 2019). During the glacial retreat, sediment yields increase dramatically, often causing stark and abrupt changes in the landscape, i.e., paraglacial adjustment (Hedding et al. 2020, Williams and Koppes 2019). Non-fluvial deposits associated with previous glaciation may also play a role in the development of channel patterns in fluvially dominated stretches (Hauer and Pulg 2018). In order to account for the decisive effects of (past) glaciation on river and valley formation, the associated semi- and non-fluvial processes acting in postglacial areas must be better included in the analyses of channel evolution (Hauer and Pulg 2021).

This calls for an integrative analysis of river morphology, including a river's geological history and wider morphological context. This need is met with the development of holistic frameworks for the morphological assessment and classification of river systems that try to take into account all associated processes on a catchment scale (e.g., Rinaldi et al. 2016, 2015). Methods like the landscape reading approach (Fryirs and Brierley 2012) aim to relate large-scale landscape features with the region's geological history. It has been adapted and applied by Hauer et al. (2021) to assess paraglacial adjustments and the quaternary development of the river Vjosa highlighting how combined morphological understanding of channel patterns can be used to explain glacially influenced river morphology. These approaches are usually based on large-scale parameters like channel width, or valley width, which are most efficiently assessed using remote sensing techniques.

Remote sensing methods are applied to assess river morphological characteristics across various spatial and temporal scales (Boothroyd et al. 2021, Piégay et al. 2020, Tomsett and Leyland 2019, Hemmelder et al. 2018) as a cost-effective monitoring tool (Bechter et al. 2018) that can help to increase objectivity and comparability (Zhao et al. 2019). They are particularly useful for assessing recent river morphological changes (Langat et al. 2019). Different methodologies have been developed that allow analysing, inter alia, changes in river morphology (Shahrood et al. 2020), river morphological status (Bechter et al. 2018), physical habitat and river health (Zhao et al. 2019), and even river gauging (Hou et al. 2020) based on remote sensing data.

Having established that morphological reference data (e.g., from 'least-disturbed' sites) can serve as valuable environmental guiding principles and support efficient, effective, and sustainable restoration measures (Kujanová and Matouškova 2017, Hey 2006, Newson and Large 2006) while acknowledging that it is next to impossible to find such sites in many regions of the world, like the European Alps (Comiti 2012), we can agree that reference sites must be found elsewhere. 'Least-disturbed' reference sites are not necessarily devoid of any signs of human activity but have suffered the least anthropogenic disturbance within a group of comparable sites (Stoddard et al. 2006). Such regions still exist in less densely populated parts of the world: Anthropogenic impacts in the Altai Mountains, for example, are minimal compared to mountain regions like the European Alps (Volkov et al. 2021). Analyses of such remote areas, especially, rely largely on remotely sensed data.

This study focuses on the morphology of the mountain river Biya in the Russian Altai region (Siberia), which can be regarded as an example of a morphologically least-disturbed river. This river has been studied regarding hydrological properties (Chalov and Ermakova 2011) as well as its geological origins (Baryshnikov et al. 2016). Our study aims to analyse the relationship between the Biya catchment's geological history and its morphological characteristics, described using remotely sensed data based on clearly defined morphological parameters. Following the approach described by Hauer et al. (2021), it shall be illustrated how the evolutionary history of the Biya's different river stretches is reflected by their morphology.

MATERIALS AND METHODS

The study area

The study at hand focuses on the river Biya, one of the two headstreams of the river Ob. The Biya's catchment lies in the Russian part of the Altai Mountains in Siberia (Schletterer et al. 2021). Siberia accounts for 80% of all global freshwater resources, as three of the world's largest and longest rivers (Lena, Yenisei, and Ob) originate there (Klubnikin et al. 2000). The Altai Mountains are among the least disturbed natural areas worldwide and can be considered a center of biological diversity (Dirin and Madry 2017). The area is particularly important for conserving unique habitats characteristic of the Central Asian Mountain System (Chlachula and Sukhova 2011). The area north of Lake Teletskoye, in particular, is reported to have served as a refuge for deciduous plant species during the last glacial maximum (LGM, Hais et al. 2015).

The Biya's origin (Fig. 1A) lies at the outflow of Lake Teletskoye (51°47'13"N, 87°14'49"E, 430 m a.s.l., near the city of Artybash), which is Russia's second deepest natural lake (Dehandschutter et al. 2002). The Biya covers a distance of 301 km until its confluence with the Katun (52°26'12"N, 85°0'47"E, 160 m a.s.l., near the city of Biysk). It has a catchment of about 36,900 km^2. Close to the city Biysk, about 21 km upstream of its confluence with the Katun,

the Biya has an average annual discharge[1] of 476 m^3/s. The chainage information in the following is presented as river kilometres (rkm) starting with 0 at the outflow of Lake Teletskoye. The Biya can be divided into the following three parts: upper Biya (Lake Teletskoye to the mouth of the river Lebed', rkm 0-86) – middle Biya (river Lebed' to Lebyaj'e, rkm 86-196) – lower Biya (Lebyaj'e to the confluence with the Katun, rkm 196-301; sub-stretch division based on *Surface water resources of the USSR 1962*). The most important headstream of the Biya is the Chulyshman (Fig. 1A). Fig. 1C includes additional information on grain size distribution from a Wolman pebble count (Wolman 1954) at three sites along the Biya (Artybash, Kebezen, and Biysk; data kindly provided by Friedrich Seidl). The photographs in Fig. 1B give an impression of the conditions on-site.

In order to discuss hydromorphological processes along a river, it is important to know the river's geomorphological history, which is dependent on its geological setting. The geomorphological development of the Biya valley has, however, not been studied as thoroughly as that of other rivers in the Altai mountains, such as the Katun and the Chuya (e.g., Baryshnikov 2016, Zolnikov et al. 2016, Zolnikov et al. 2015, Baker et al. 1993, Rudoy and Baker 1993). While the Katun still follows its ancient initial course, the Biya, which used to be a small river in the early middle Pleistocene, has grown in length since then: The Biya valley between Lake Teletskoye and the village Turochak (around rkm 75) was formed only in late middle Pleistocene following the beginning of the outflow from the lake. This uppermost part can be described as a mountain river. The lower stretch downstream of Turochak is a well-developed alluvial valley, probably dating back to pre-Quaternary times (Baryshnikov et al. 2016).

In the Biya valley, distinct traces of large-scale flood events can be found: Giant current ripples bear witness to past megafloods caused by glacial lake outburst (Baryshnikov 2016, referring to Baryshnikov 1979). Moraine dam failure caused the catastrophic Biya debris flow (BDF) which initiated the valley incision processes that led to abrupt morphological changes and the development of the river Biya about 37.5 ka before present (Baryshnikov et al. 2016).

Morphological Characterisation

The hydromorphological characterisation of the river Biya was based on the landscape reading approach described by Hauer et al. (2021). This approach aims

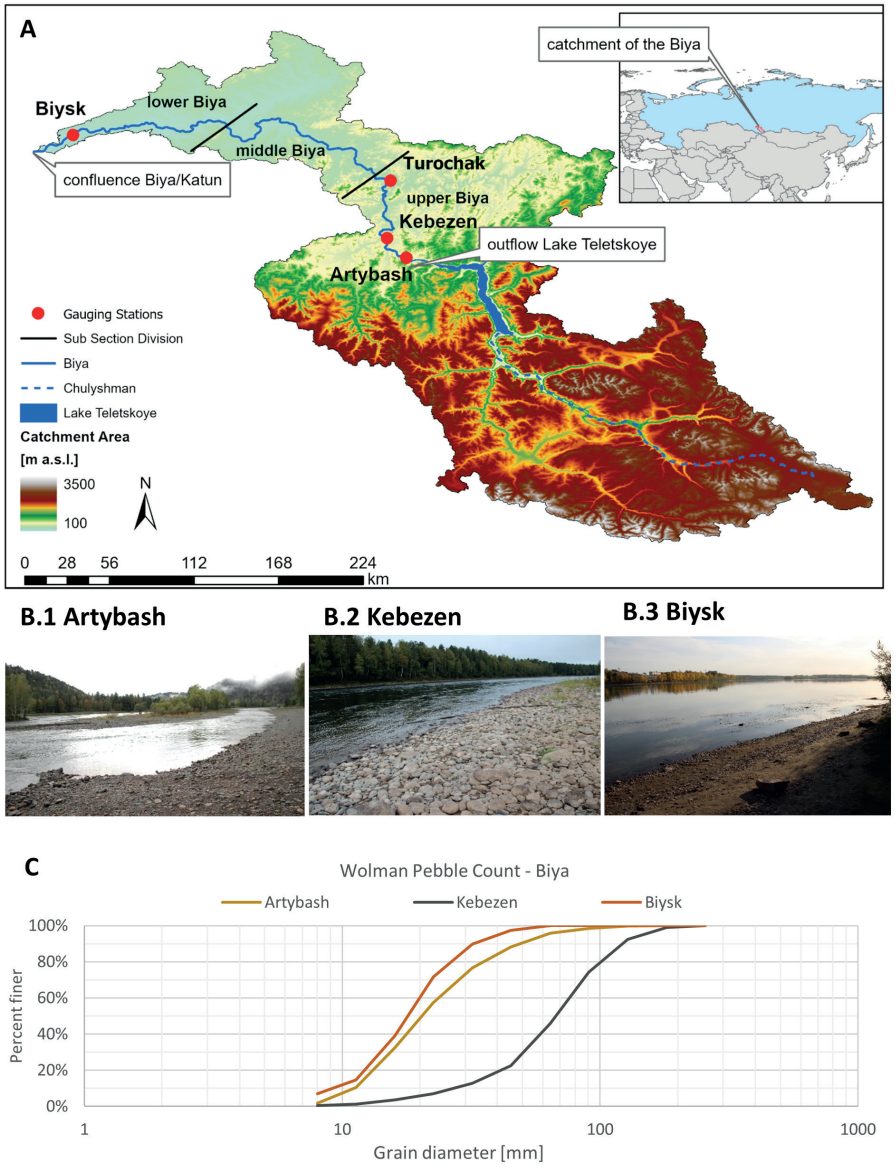

Fig. 1. A: Overview: Catchment of the river Biya. The locations of the four gauging stations are marked in red. Black lines indicate the starting/ending points of upper, middle and lower sections. B: Grain size sampling sites (Artybash, Kebezen, Biysk). Photographs by Martin Schletterer. C: Grain size distribution curves

[1]Russia ArcticNET: https://www.r-arcticnet.sr.unh.edu/v4.0/ViewPoint.pl?Point=6670

to develop an understanding of the morphological background of the area of interest (Fryirs and Brierley 2012). It requires the following three parameters: Active Channel (AC), Active Floodplain (AF), and Morphological Floodplain (MF). While AC and MF were determined during the GIS survey, AF was established from a hydraulic 1D step-backwater model (HEC-RAS) of a flood scenario with a five-year-recurrence interval (HQ5) based on Hauer et al. (2021). In this approach, AF is defined as the wetted cross-section width in the HQ5 scenario. The HQ5 scenario was determined using the long-time data series (*Russia ArcticNET*[1]) for four gauging stations based on a Gumbel distribution (Yue et al. 1999). Channel sinuosity (see below) was added to this set of parameters to allow for a more comprehensive evaluation of the Biya's hydromorphological characteristics. Further differentiation between hydraulic and topographic sinuosity was undertaken to visualise the interactions between the planform river pattern and the surrounding terrain. Next to a geographic characterisation, hydrological and geological boundary conditions were established based on published literature and online data sources (see details below).

A supplementary catalogue of hydromorphological characteristics was established for thirty 10 km-stretches (300 km in total) along the Biya. It is presented as an overview table (Appendix: Tables A.1-3), documenting the morphological variability occurring in a least-disturbed river system. A verbal discussion of the changes in channel characteristics in relation to the surrounding topography emphasises the importance of a holistic approach in applying hydromorphological reference parameters. It is targeted that the results may be used as a basis for ecological guiding principles for river restoration planning in the European Alps.

Hydrological Information

Hydrological information for four gauging stations along the river Biya was taken from the platform *Russia ArcticNET*[2], where monthly discharge values are given for at least three decades. The gauging stations are located at Artybash (rkm 2), Kebezen (rkm 30), Turochak (rkm 81), and Biysk (rkm 280).

GIS Survey

As a first step, the required geometric information was generated and compiled: For this study, remote sensing data represented the most valuable input. Topographic information from ASTER GDEM v3 (Advanced Spaceborne Thermal Emission and Reflectance Radiometer Global Digital Elevation Model, Version 3[3]) was used. The geometric attributes needed for this study were established in ArcMap (ESRI: ArcGIS Desktop 10.8.1) based on ASTER GDEM. Inputs for the analysis of planform morphological parameters (i.e., river axis, active channel width, valley cross-sections and valley width) were largely delineated manually, combining topographic information with recent satellite images. A longitudinal section of the river axis was extracted. Special focus in this study was placed on channel sinuosity.

Sinuosity Calculations

Channel sinuosity is an indicator of the meandering intensity of a river, which is commonly evaluated by a sinuosity index (Mueller 1968). The standard sinuosity index (SSI) quantifies the ratio of the channel length to valley length:

$$SSI = \frac{CL}{VL} \tag{1}$$

where *CL* = channel length, and *VL* = valley length (here: the average between the length of the left and right valley flank).

The total sinuosity of a river is always a combination of hydraulic (i.e., controlled by the river's flow through its flood plain) and topographic (i.e., determined by the shape of the surrounding landscape) sinuosity (Mueller 1968). These two parameters are quantified by the hydraulic (Eq. 2: *HSI*) and topographic (Eq. 3: *TSI*) sinuosity index (calculated based on *CL, VL*, and linear distance, *LD*, between starting and end point of each subsection). Per definition, *HSI* and *TSI* can be added to a total of 1.

$$HSI = \frac{\frac{CL - VL}{LD}}{\frac{CL}{LD} - 1} \tag{2}$$

$$TSI = \frac{\frac{VL}{LD} - 1}{\frac{CL}{LD} - 1} \tag{3}$$

All three sinuosity indices were calculated based on the manually delineated river axis (*CL*) and visually obtained valley borders. The river axis was divided into subsections of 10 km length for which the calculations were performed.

Statistical Testing

All statistical tests were done in R-4.1.1 (R core team, 2021). Differences between the river stretches regarding the landscape reading elements (AC, AF, MF) were assessed with Wilcoxon rank sum tests. Comparisons between all observed parameters (incl. *SSI, HSI/TSI,* and slope) were based on regression analyses using average values for stretches of 10 km length.

RESULTS

For the morphological analyses, the established river stretches (upper Biya: rkm 0-86, n = 85 – middle Biya: rkm 86-196, n = 109 – lower Biya: rkm 196-301, n = 108) were kept. AC, AF, and MF were assessed based on a cross-sectional view at 1 km increments (n =302). Sinuosity values (*SSI, HSI*, and *TSI*) were calculated for stretches of 10 km length (n = 30). The division between upper and middle Biya (and middle and lower Biya) was, in this case, set at rkm 90 (and rkm 200, respectively; $n_{upper} = 9$; $n_{middle} = 11$; $n_{lower} = 10$). The performed analyses (landscape reading elements, hydraulic/topographic sinuosity, and longitudinal profile) show a clear distinction between the upper Biya and the other two sections (Fig. 5), reflecting the differences in the evolutionary history of the upper

[1]Russia ArcticNET: https://www.r-arcticnet.sr.unh.edu (see specifications above)
[2]Russia ArcticNET (Point IDs XXX : 6929 Artybash – 6668 Kebezen – 6669 Turochak – 6670 Biysk):
https://www.r-arcticnet.sr.unh.edu/v4.0/ViewPoint.pl?View=ALL&Unit=ms&Point=XXXX
[3]EarthData: earthdata.nasa.gov, provided by NASA (National Aeronautics and Space Administration) and freely available

river stretch. The statistical analyses showed a relationship between MF and sinuosity (both *SSI* and *HSI/TSI*). Tab. 2 gives an overview of all observed morphological parameters for the upper, middle, and lower Biya. The slope decreases in the downstream direction: While the upper Biya has an average slope of 1.56‰, the gradient of the middle Biya lies only at 0.88‰ and is as low as 0.36‰ in the lower stretch. *SSI* does not show any specific trend. It remains, on average, within the sinuous range (1.06 to 1.25, Brice 1982) for all three stretches. *HSI* and *TSI*, in contrast, show clear increasing (respectively decreasing) tendencies in the downstream direction.

Fig. 2A shows the longitudinal section of the Biya from its origin at Lake Teletskoye down to its confluence with the Katun, separated into upper, middle, and lower stretch. Over a length of about 301 km, the Biya travels roughly 270 m downstream at an average slope of 0.9‰ (compare to sectional slope in Table 2). The locations (river station and orographic side) of all 24 tributaries (*from Russian Water Register*[1]) are indicated in the graph. Additionally, the mean annual discharge at the four gauging stations (Artybash, Kebezen, Turochak, and Biysk, from *Russia ArcticNET*[2]) is included.

Fig. 2B illustrates the development of the three landscape reading elements plus SSI values along the river. SSI is highest where MF peaks. A direct comparison of AC and AF suggests lateral dynamics in the upper Biya are restricted compared to the middle and lower stretch. In the upper stretch, the mean differences between AC and AF amount to 157.45 m, on average, which is less than the mean AC width of 226.82 m. In comparison, differences between AC and AF in the middle and lower Biya come to 532.78 m and 677.95 m, respectively, in both cases exceeding the mean AC widths. This suggests a higher influence of the surrounding topography in the upper Biya.

Fig. 2C shows the ratio between *HSI* and *TSI*. Since HSI and TSI add up to a total of 1, those two values are presented as a stacked bar chart. Hydraulic sinuosity outweighs topographic sinuosity for most of the Biya's length, showing an increasing tendency in downstream direction.

In the upper section (rkm 0-86), the river's valley runs in a rather straight course from south to north (Fig. 3). Over the first 50 km, *HSI* and MF increase rather steadily. Along the upper Biya *SSI* and *HSI* exhibit analogue patterns that correlate visibly with MF values (Fig. 2B and C).

The middle Biya flows towards the northwest over a less mountainous terrain than the upper course. Overall, both valley and river axis show a more complex, winding pattern than in the upper stretch. Three tributary mouths are located within the first ten kilometres of the middle Biya (rkm 86-196). Interestingly, this correlates with an increase in *HSI*, but not in MF. Near rkm 110, the whole valley turns westward, coinciding with a visible drop in *HSI*, indicating topographic constraints. A local peak in *TSI* (rkm 100-110: 80.04%) precedes another peak in HSI (rkm 150-160: 97.91%) which is followed by a reduction in MF (between rkm 160 and rkm 180) and a decrease in HSI that continues until the start of the Biya's lower stretch.

The lower stretch of the Biya (rkm 196-301) starts out with a *TSI*-dominated section (rkm 200-210: 95.81%), after which *SSI*, alongside MF, reaches its peak between rkm 210-220 at the confluence between the Biya and its tributary Souskanikha. *HSI* increases after that local minimum and remains high for most of the remaining lower stretch.

One special focus of the study was the evaluation of channel sinuosity. The goal was to relate sinuosity parameters (*SSI, HSI/TSI*) to the other morphological key parameters. Fig. 3 shows the SSI values for each 10 km-section along the Biya in plan view. Only four stretches (rkm 60-70: 1.55 – rkm 150-160: 1.55 – rkm 160-170: 1.53 – rkm 210-220: 1.74) lie above 1.5. These stretches occur in all three sections of the Biya, one each in the upper and lower stretch, and two adjoining 10 km sections in the middle Biya. None of the three stretches differ significantly from one another regarding sinuosity (SSI, Fig. 5D, mean values: upper: 1.21, middle: 1.18, lower:1.23). The number of observations (n between 9 and 11) is, however, quite low for making statistically meaningful statements. There is a wider range of *SSI*-values occurring in the lower Biya (1 to 1.74), than in the upper stretch (1 to 1.55) with *SSI* values in the middle stretch ranging from 1.02 to 1.55 (Fig. 2B and Fig. 5D).

Next to the planform channel pattern (i.e., considering the x and y dimension), the longitudinal elevation of the three stretches of the Biya was analysed. In contrast to the middle and lower stretch, the upper Biya's longitudinal elevation profile can best be approximated by a linear equation ($R^2 = 0.9827$), while for the other two, a quadratic polynomial equation provides a better fit (Fig. 4).

Fig. 2 shows that the upper, middle, and lower Biya exhibit different morphological characteristics. These are confirmed by the statistical differences between the observed parameters (Fig. 5). Pairwise comparisons between all three stretches were performed using the Wilcoxon rank sum test to test for significant differences

MF (Fig. 5A) differs significantly between all three stretches of the Biya. The difference in MF between the upper Biya (mean: 1866.42 m) and both the middle (mean: 3521.16 m) and lower (mean: 4236.82 m) Biya can be described as highly significant ($p < 0.001$). MF in the middle and upper Biya still differs significantly ($p = 0.002$). AF (Fig. 5B) within the upper Biya (mean: 384.28 m) also shows highly significant differences ($p < 0.001$) from the other two stretches. There is, however, no significant difference between the middle (mean: 955.83 m) and the

Table 2. Elevation and (average) slope, widths of active channel (AC), active floodplain (AF), and morphological floodplain (MF), including standard (SSI), hydraulic (HSI), and topographic (TSI) sinuosity index for the upper, middle, and lower Biya

	River Kilometer		Slope	AC	AF	MF	SSI	HSI	TSI
	Start	End	Average	Average			Average		
	[km]	[km]	[‰]	[m]	[m]	[m]	[-]	[%]	[%]
Upper	0	86	1.56	227	384	1866	1.21	56	44
Middle	86	196	0.88	423	956	3521	1.18	64	36
Lower	196	301	0.36	373	1051	4237	1.23	69	31

[1]Russian Water Register: http://textual.ru/gvr/index.php?card=187196
[2]Russia ArcticNET: https://www.r-arcticnet.sr.unh.edu (see specifications above)

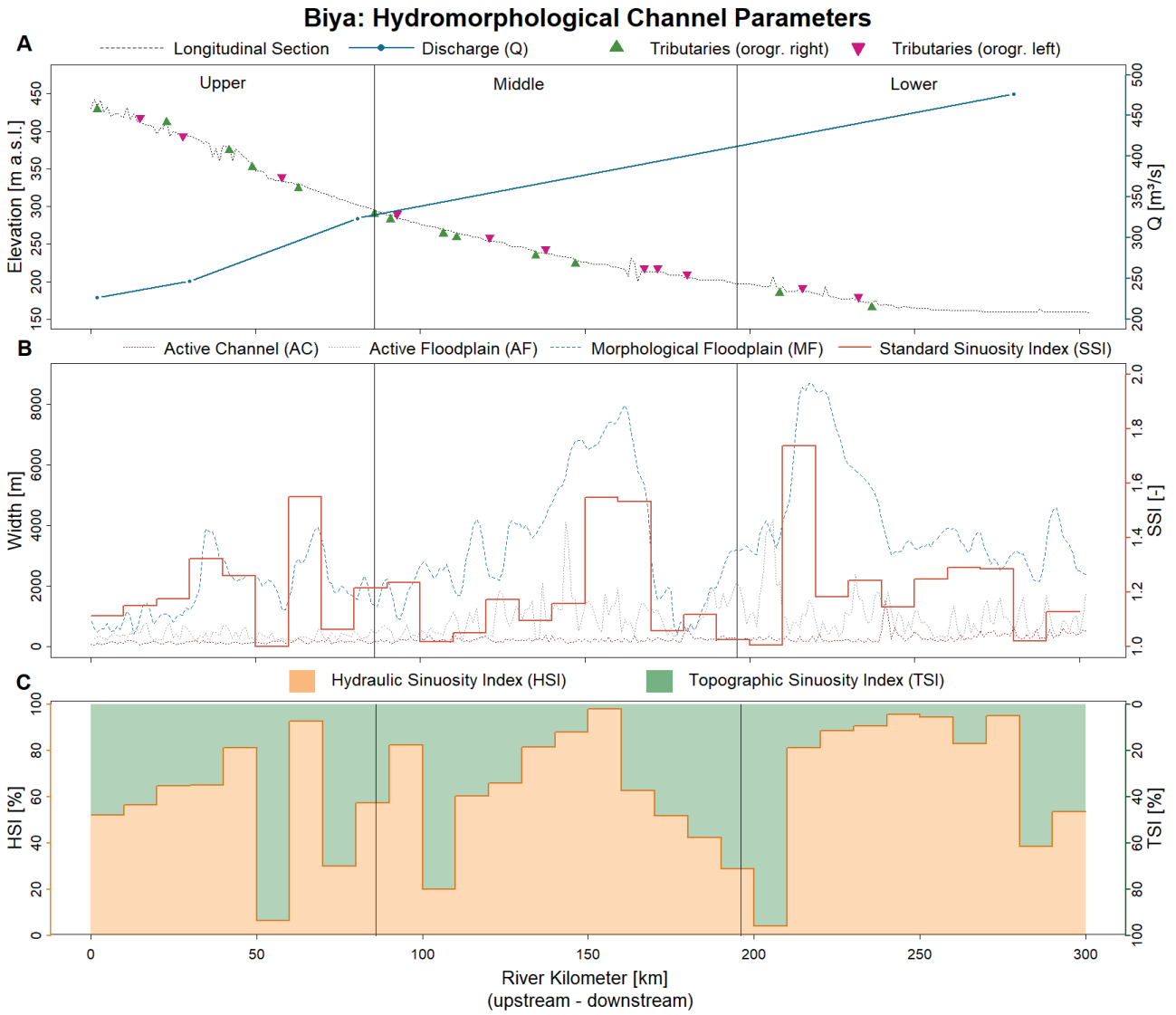

Fig. 2. Overview of the assessed morphological parameters along the Biya. A) Hydrological overview in longitudinal section: Discharge (Q) and tributaries. B) Landscape reading elements (widths of the active channel, AC, active floodplain, AF, and morphological floodplain, MF) incl. standard sinuosity index (*SSI*). C): Hydraulic (*HSI*) vs. topographic (*TSI*) sinuosity index. *HSI* values (orange) can be read on the left-hand y-axis, starting at the bottom with a value of zero. *TSI* values (green) are given on the right-hand y-axis, starting at the top with zero

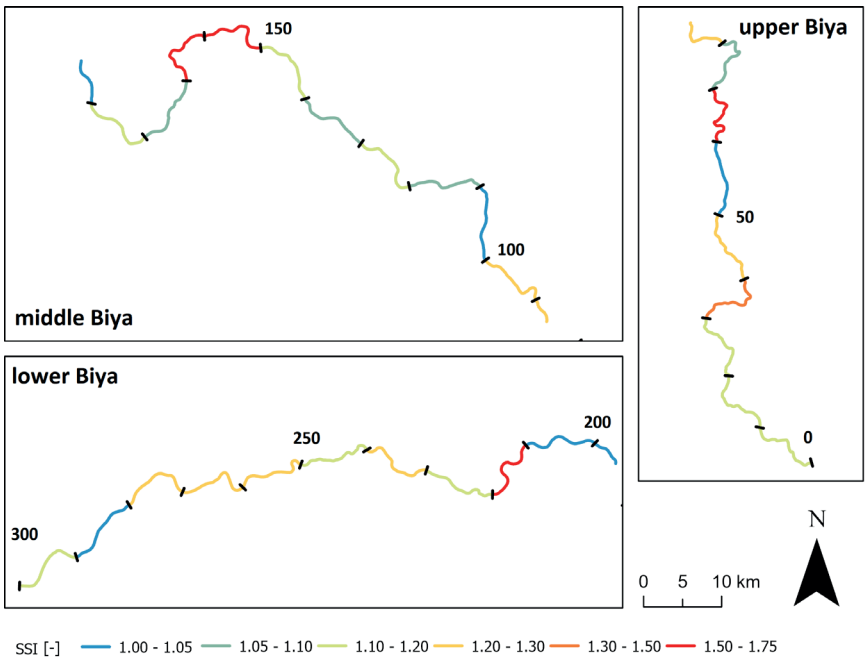

Fig. 3. Plan view of the river Biya including *SSI* values for 10 km sections

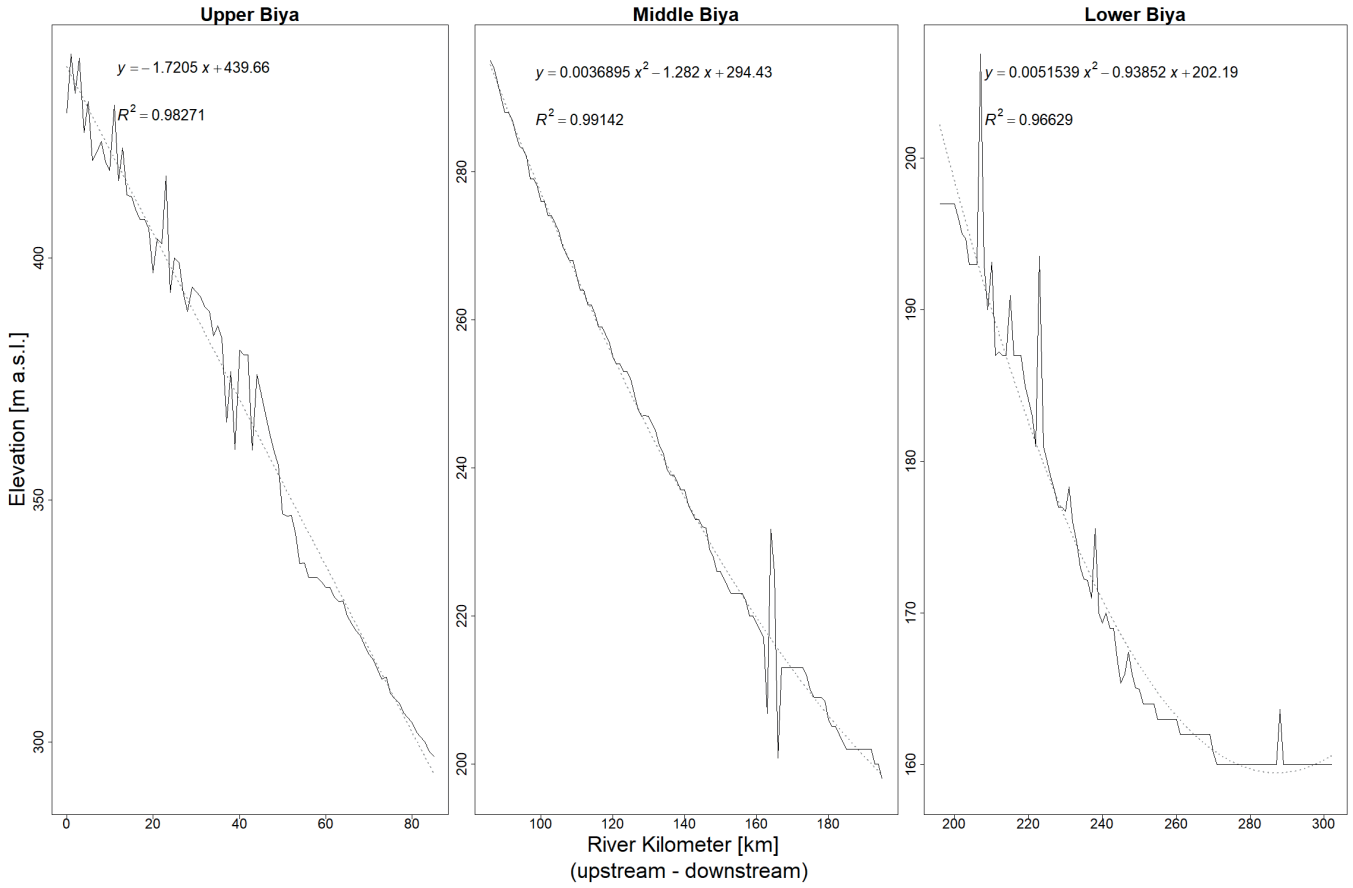

Fig. 4. Longitudinal profiles of the upper, middle, and lower Biya

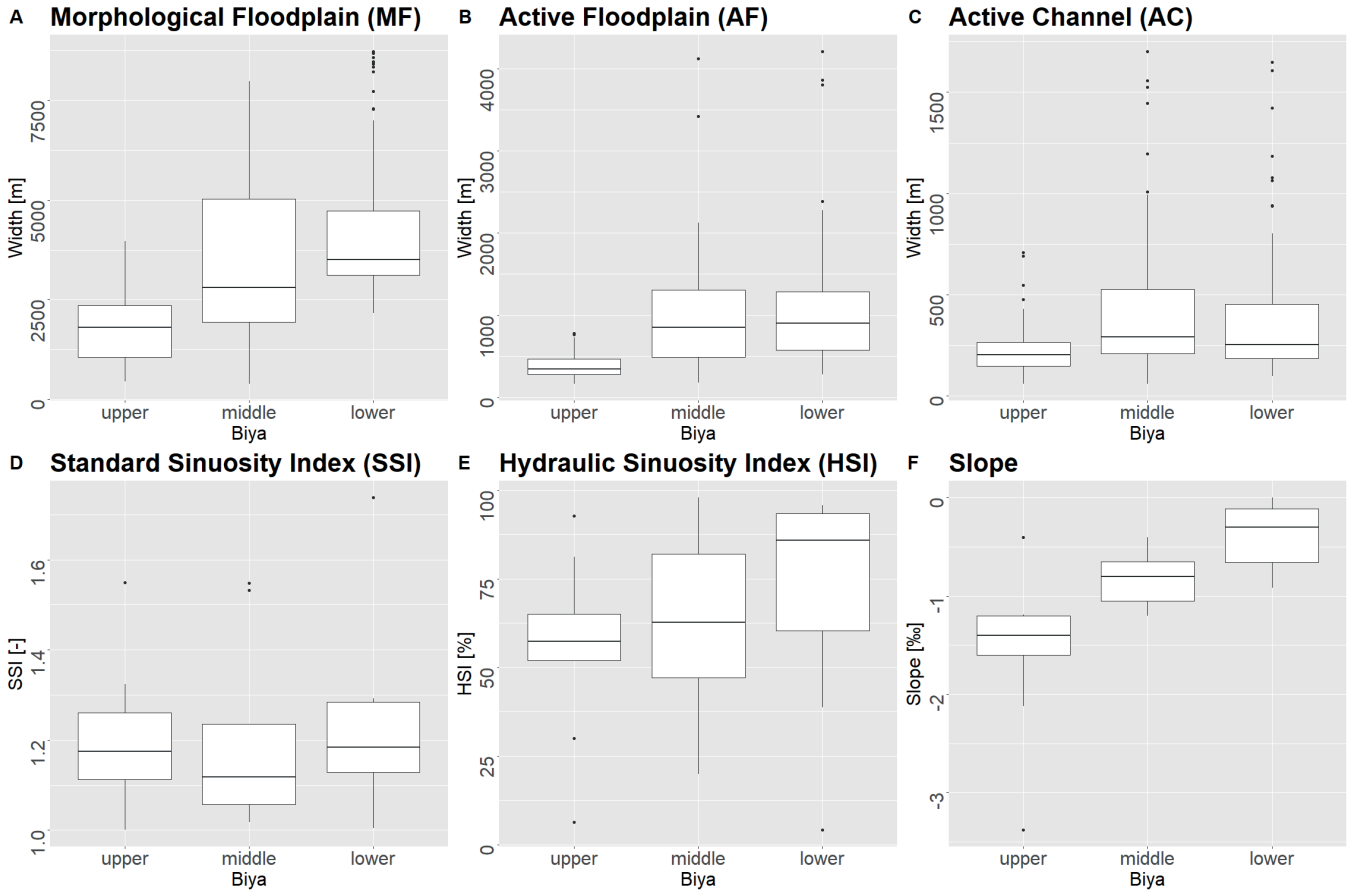

Fig. 5. Boxplots of the assessed morphological parameters

lower (mean: 1051.31 m) Biya regarding AF ($p = 1$). The statistic differences in AC (Fig. 5C) behave similarly: The upper Biya (mean: 226.82 m) differs from the other two stretches at highly significant levels ($p < 0.001$), while there is no significant difference ($p = 0.5$) between AC widths within the middle (mean: 423.06 m) and lower Biya (mean: 373.36 m). Within each of the three stretches, MF, AF, and AC all show highly significant differences from one another ($p < 0.001$).

Regression analyses with all observed parameters (AC, AF, MF, *SSI*, *HSI/TSI*, and slope) were performed using data that had been averaged for stretches of 10 km length. Fig. 6 shows a pairwise arrangement of these values plotted against each other. In most cases, no distinct (linear) relationship could be identified.

Based on these initial analyses (Fig. 6), correlations between MF and sinuosity (*SSI*, and *HSI/TSI*) were suspected. These three relationships are presented in more detail in Fig. 7. As could be expected, higher *SSI* values correlate with higher HSI values (and lower *TSI* values, respectively). Channel 'maturity' (indicated by the ratio between *HSI* and *TSI*, with higher *HSI* values suggesting a more 'mature' stage of the river and a better developed floodplain) is closely related to MF width. Accordingly, higher *HSI* values were also associated with higher MF values. In all cases, the coefficient of determination (R^2) is rather weak: The strongest linear relationship could be identified between *SSI* and *HSI* ($R^2 = 0.37$). The relationships between MF and *SSI* (and MF and *HSI*) are explained by linear regression at R^2 levels of 0.29 (and 0.19, respectively).

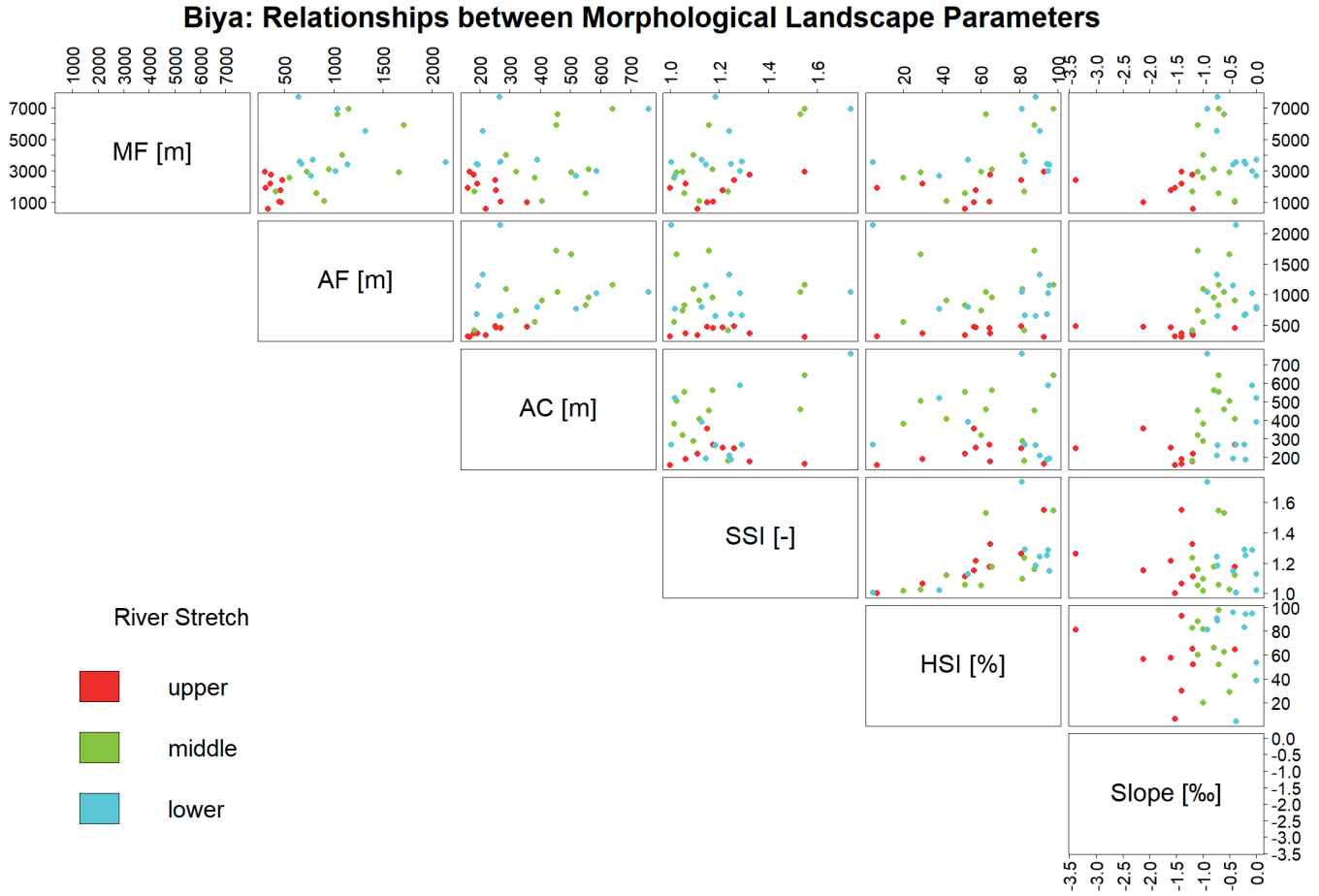

Fig. 6. Regression analyses for the assessed morphological parameters

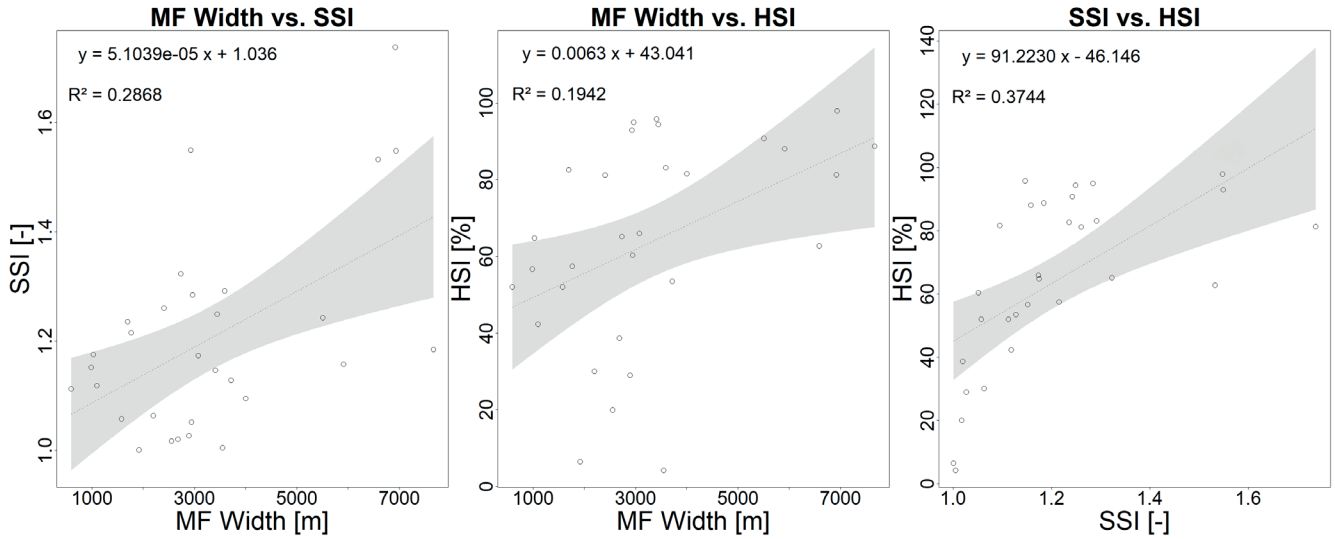

Fig. 7. Linear regression models for the relationships between MF, *SSI*, and *HSI*

DISCUSSION

The appearance and shape of a natural river result from complex morphological processes and interactions, majorly influenced by geological factors and climatic and hydrological controls (Mahala 2020, Castro and Thorne 2019, Stepinski and Stepinski 2005). These boundary conditions define sediment dynamics and determine the interactions between a river and its surrounding topography (Ibisate et al. 2011). Therefore, a profound understanding of a river's geological history is of utmost importance. Periods of glaciation, for example, that date back several thousands of years have strong impacts on today's rivers since glacial processes have provided large quantities of moraine material that gradually enters the sediment cycle (Sokołowski et al. 2021, Huang et al. 2019). Other processes associated with glaciation include the development of glacial lakes that can accumulate large volumes of lacustrine sediments, which may be released through rivers draining these lakes (Baryshnikov 2016). The temporal scale of the associated processes ranges from long-term deposition of lake sediments to rapid onset release events, like glacial lake outburst floods (GLOFs). The after-effects of certain climatic conditions can extend over millennia, so it is essential to consider the whole geological background when assessing a river's morphology. The evaluation of channel sinuosity alongside morphologically significant width parameters (AC, AF, MF) in this study has highlighted the influence of the different geological histories on the morphological characteristics of the upper Biya compared to the middle and lower stretch. The results confirm a distinction based on morphological history and show how different morphological river characteristics result from a river's geological past.

Glaciation and climatic history of the Altai mountains have been described in great depth (Blomdin et al. 2018, Blomdin et al. 2016, Chernykh et al. 2014, Agatova et al. 2012, Surazakov et al. 2007). The Altai mountains have been the scene of some of the largest freshwater megafloods that are known in planetary history (Herget et al. 2020, Bohorquez et al. 2019, Carling et al. 2002, Rudoy 2002). The most recent glacial activity during the Altai mountains' latter half of the holocene seems to have taken place simultaneously with those in the European Alps (Chernykh et al. 2013). It is reported that the maximum extent of glaciation reached the Biya's origin at Lake Teletskoye (Lehmkuhl et al. 2004). As of 2008, only 6.9 km^2 of the Biya's catchment are glaciated, with a clear decreasing tendency (Narozhniy and Zemtsov 2011).

The basin formation of Lake Teletskoye was not caused by quaternary glaciation. The Teletsk graben developed very recently (starting in the Pleistocene) in the contact zone between two Paleozoic blocks as a consequence of shear zone reactivation (Dehandschutter et al. 2002, De Grave and Van den Haute 2002). The formation of the actual lake was, however, a consequence of glacial retreat (about 37.5 ka before present), leaving a moraine-dammed lake (Baryshnikov et al. 2016). The complex tectonic conditions in the upper Biya valley determine the river's outflow direction (Baryshnikov 2016) thereby acting as controls on the course of the river.

Valley shape and different levels of confinement develop in relationship with various geological processes (Fryirs et al. 2016). Measures of confinement and valley width can be used to infer a river's geological history and to interpret its future development (Fryirs et al. 2016 referring to Fryirs and Brierley 2010 and Brierley and Fryirs 2015). Channel sinuosity is often strongly influenced by topographic constraints like valley margins (Woolderink et al. 2021, Fryirs and Brierley 2010, Tímar 2003), acting as a fundamental control on river character and behaviour (Fryirs et al. 2016). Including channel sinuosity and especially TSI in morphological analyses can help to identify interactions between river geometry and such topographic restraints. At the river Biya, high HSI values were associated with higher MF values (i.e., wider valley cross-sections). In this study, the dependence of channel curvature on topographic constraints (indicated by TSI) was shown to decrease in downstream direction, indicating an increasing stage of the river's 'maturity'.

The upper Biya (between Lake Teletskoye and Turochak) has been described as the least developed and narrowest section (Baryshnikov et al. 2016) with mountain river character (Baryshnikov 2016). It was only formed in the late middle Pleistocene when the outflow from Lake Teletskoye began. The remaining part, a well-developed valley is much older (probably dating back to the pre-Quaternary period, Baryshnikov et al. 2016). It could be shown that the upper Biya differs significantly from the other two stretches based on morphological parameters (AC, AF, MF). Glacial processes have determined the morphology of the upper Biya (Baryshnikov et al. 2016). The glacier that used to run through the basin of Lake Teletskoye contributed significantly to sediment production (Baryshnikov 2016). Lacustrine sediment deposits from glacial lakes in the upper Biya's tributary valleys and glacial moraine deposits along the main valley also supplied substantial amounts of sediment. A phase of rapid channel incision of the upper Biya was triggered by a cataclysmic glacial lake outburst event originating from Lake Teletskoye (about 37.5 ka before present, Baryshnikov et al. 2016). This incision into the alluvion is reflected by the limited extent of the active floodplain and restricted lateral dynamics in the upper stretch, indicating a higher sediment supply during the glacial period (Williams and Koppes 2019). The applied method already yielded similar findings at the Vjosa (Hauer et al. 2021). After the rapid incision triggered by the BDF, valley deepening rates slowed to about 0.8-0.9 m per thousand years (Baryshnikov et al. 2016). The upper Biya exhibits a linear longitudinal profile, while the middle and lower Biya follow a concave shape best described by a quadratic polynomial equation. The linear profile is associated with an equilibrium between sediment supply and transport without downstream fining. In contrast, the concave longitudinal profile in the lower Biya is an indicator for downstream fining and channel aggradation (Rice and Church 2001, referring to Mackin 1948). The elevation peaks in the longitudinal profiles (Fig. 4) are most likely caused by uncertainties in the delineation of the channel axis. These errors do, however, not alter the overall characteristic of the longitudinal profile shape of the three sub-stretches.

It could be demonstrated that the upper Biya, which is known to have a different geological background than the middle and lower part (Baryshnikov et al. 2016), significantly differs from the other two stretches based on morphological parameters (AC, AF, MF). The results clearly show that the relatively simple landscape reading approach, according to Hauer et al. (2021), which relies on only three width parameters on a cross-sectional basis, was able to account for the differences in the evolutionary history between the upper Biya and the two remaining sections. This is of particular interest since these parameters are clearly defined and comparably easy to obtain – allowing for a standardised differentiation between river stretches based on their morphological history. The fact that SSI could not be used to explain the differences in channel

evolution between the upper Biya and the remaining river stretch was interpreted as an indicator that the focus should rather be placed on the determining factors behind channel sinuosity and include the wider morphological context. Both the landscape reading approach (after Hauer et al. 2021) and the consideration of hydraulic and topographic sinuosity (after Mueller 1968) have proven useful in this regard.

The most striking constraint to the performed channel pattern analyses was the resolution of the input data at a cell size of 30 m by 30 m. Additional uncertainties within the lowermost 70 km must be mentioned, where catchment borders close in on the river axis and the extent of the morphological floodplain is hard to identify.

Comprehensive assessment of river landscape parameters is a key factor for developing a profound understanding of the complex multi-scale processes operating along and within a river system (see also the review of riverscape approaches by Torgersen et al. 2022). This is especially important when establishing environmental guiding principles and aiming to transfer these observations to other, more heavily disturbed systems. For this purpose, a supplementary catalogue of morphological parameters and verbal descriptions could be established for 10 km stretches along the whole Biya. This comprehensive set of parameters is summarised in Tables A.1-3 (see Appendix).

CONCLUSIONS

In this study of the alpine river Biya, the morphological parameters of a river in the least-disturbed condition were assessed and put into context with its geological history. The concept of 'reading the landscape' (Fryirs and Brierley 2012) in a hybrid approach, including measuring and hydrodynamic-numerical modelling (Hauer et al. 2021) was applied to differentiate between upper, middle, and lower Biya. The study could confirm the differentiation between the upper Biya and the rest of the river based on the different channel evolution history, highlighting the relationship between geological history and channel morphological parameters. Contrary to the initial expectations, channel sinuosity (*SSI*) could not be used to divide the Biya into morphologically meaningful sub-stretches. MF could best explain the differentiation between upper, middle, and lower Biya. The statistical analyses showed a relationship between MF and sinuosity (both *SSI* and *HSI/TSI*). The results of this study confirm that easily obtainable parameters (AC, AF, and MF) can be used to detect differences in the morphological history of river stretches, as was already shown for the Vjosa (Hauer et al. 2021).

REFERENCES

Anderson S.W. and Konrad C.P. (2019). Downstream-propagating channel responses to decadal-scale climate variability in a glaciated river basin. Journal of Geophysical Research: Earth Surface, 124(4), 902-919, DOI: 10.1029/2018JF004734.

Abily M., Acuña V., Gernjak W., Rodríguez-Roda I., Poch M. and Corominas L., (2021)' Climate change impact on EU rivers' dilution capacity and ecological status. Water Research, 199, 117166, DOI: 10.1016/j.watres.2021.117166.

Agatova A.R., Nazarov A.N., Nepop R.K. and Rodnight H. (2012). Holocene glacier fluctuations and climate changes in the southeastern part of the Russian Altai (South Siberia) based on a radiocarbon chronology. Quaternary Science Reviews, 43, 74-93, DOI: 10.1016/j.quascirev.2012.04.012.

Baker V.R., Benito G. and Rudoy A.N. (1993). Paleohydrology of late Pleistocene superflooding, Altay mountains, Siberia. Science, 259(5093), 348-350, DOI: 10.1126/science.259.5093.348.

Baryshnikov G.Y. (2016). Geological and geomorphological background of cataclysmic debris flooding in the Altai mountain rivers. Geography and Tourism, 4(2), 75-81, DOI: 10.5281/zenodo.223926.

Baryshnikov G.Y., Panin A. and Adamiec G. (2016). Geochronology of the late Pleistocene catastrophic Biya debris flow and the Lake Teletskoye formation, Altai Region, Southern Siberia. International Geology Review, 58(14), 1780-1794, DOI: 10.1080/00206814.2015.1062733.

Baryshnikov G.Y. (1979). Revisiting the formation of debris-flow sediment in the Biya valley. Geology and Mineral Resources in Altai Region. Altai University Press, Barnaul, 117-119. (as cited by Baryshnikov 2016)

Bechter T., Baumann K., Birk S., Bolik F., Graf W. and Pletterbauer F. (2018). LaRiMo-A simple and efficient GIS-based approach for large-scale morphological assessment of large European rivers. Science of the Total Environment, 628, 1191-1199, DOI: 10.1016/j.scitotenv.2018.02.084.

Blomdin R., Stroeven A.P., Harbor J.M., Gribenski N., Caffee M.W., Heyman J., Rogozhina I., Ivanov M.N., Petrakov D.A., Walther M. and Rudoy A.N. (2018). Timing and dynamics of glaciation in the Ikh Turgen Mountains, Altai region, High Asia. Quaternary Geochronology, 47, 54-71, DOI: 10.1016/j.quageo.2018.05.008.

Blomdin R., Heyman J., Stroeven A.P., Hättestrand C., Harbor J.M., Gribenski N., Jansson K.N., Petrakov D.A., Ivanov M.N., Alexander O. and Rudoy A.N. (2016). Glacial geomorphology of the Altai and western Sayan mountains, central Asia. Journal of Maps, 12(1), 123-136, DOI: 10.1080/17445647.2014.992177.

Bohorquez P., Jimenez-Ruiz P.J. and Carling P.A. (2019). Revisiting the dynamics of catastrophic late Pleistocene glacial-lake drainage, Altai Mountains, central Asia. Earth-Science Reviews, 197, 102892, DOI: 10.1016/j.earscirev.2019.102892.

Boothroyd R.J., Nones M. and Guerrero M. (2021). Deriving planform morphology and vegetation coverage from remote sensing to support river management applications. Frontiers in Environmental Science, 9, 657354, DOI: 10.3389/fenvs.2021.657354.

Brice J.C. (1982). Stream channel stability assessment. Final Report. (No. FHWA/RD-82/021). United States. Federal Highway Administration. 44 pp.

Brierley G.J and Fryirs K. (2015). The use of evolutionary trajectories to guide 'moving targets' in the management of river futures. River Research and Applications, 32(5), 823-835, DOI: 10.1002/rra.2930.

Carling P.A., Kirkbride A.D., Parnachov S., Borodavko P.S. and Berger G.W. (2002). Late Quaternary catastrophic flooding in the Altai mountains of south–central Siberia: a synoptic overview and an introduction to flood deposit sedimentology. Flood and megaflood processes and deposits: recent and ancient examples, 17-35.

Castro J.M. and Thorne C.R. (2019). The stream evolution triangle: Integrating geology, hydrology, and biology. River Research Applications, 35, 315–326, DOI: 10.1002/rra.3421-

Chalov S. and Ermakova G. (2011). Fluvial response to climate change: a case study of northern Russian rivers. Cold Region Hydrology in a Changing Climate. IAHS, 346, 111-119.

Chernykh D.V., Zolotov D.V., Yamskikh G.Y. and Grenaderova A.V. (2014). Postglacial environmental change in the valley of Malye Chily River (the basin of Lake Teletskoye), northeastern Russian Altai. Physical Geography, 35(5), 390-410, DOI: 10.1080/02723646.2014.929881.

Chernykh D.V., Galakhov V.P. and Zolotov D.V. (2013). Synchronous fluctuations of glaciers in the Alps and Altai in the second half of the Holocene. The Holocene, 23(7), 1074-1079, DOI: 10.1177/0959683612475143.

Chlachula J. and Sukhova M. G. (2011). Regional manifestations of present climate change in the Altai, Siberia. Proc. ICEEA 2nd Int. Conf. on Environmental Engineering and Applications (Shanghai, China, August 19-21, 2011) Int. Proc. of Chemical, Biological and Environmental Engineering and Applications, 17, 134-139.

'Comiti F., Mao L., Penna D., Dell'Agnese A., Engel M., Rathburn S. and Cavalli M., (2019). Glacier melt runoff controls bedload transport in Alpine catchments. Earth and Planetary Science Letters, 520, 77-86, DOI: 10.1016/j.epsl.2019.05.031.

Comiti F. (2012). How Natural are Alpine Mountain Rivers? Evidence from the Italian Alps. Earth Surface Processes and Landforms, 37, 693-707, DOI: 10.1002/esp.226'.

De Grave J. and Van den Haute P. (2002). Denudation and cooling of the Lake Teletskoye Region in the Altai Mountains (South Siberia) as revealed by Apatite Fission-Track Thermochronology. Tctonophysics, 349(1-4), 145-159, DOI: 10.1016/S0040-1951(02)00051-3.

Dehandschutter B., Vysotsky E., Delvaux D., Klerkx J., Buslov M. M., Seleznev V. S. and De Batist, M. (2002). Structural evolution of the Teletsk graben (Russian Altai). Tectonophysics, 351(1-2), 139-167, DOI: 10.1016/S0040-1951(02)00129-4.

Dirin D. and Madry C. (2017). Transformation Processes in Traditional Nature Management Systems in the Altai Mountain Region. 17th International Multidisciplinary Scientific GeoConference, Bulgaria.

Feio M.J., Hughes R.M., Serra S.R., Nichols S.J., Kefford B.J., Lintermans M., Robinson W., Odume O.N., Callisto M., Macedo D.R. and Harding J.S. (2022). Fish and macroinvertebrate assemblages revea' extensive degradation of the world's rivers. Global Change Biology. 00, 1-20, DOI: 10.1111/gcb.16439.

Feio M.J., Hughes R.M., Callisto M., Nichols S.J., Odume O.N., Quintella B.R., Kuemmerlen M., Aguiar F.C., Almeida S.F.P, Alonso-EguíaLis P. et al. (2021). The Biological Assessment and Rehabilitation of the World's Rivers: An Overview. Water, 13, 371, DOI: 10.3390/w13030371.

Fildani A., Hessler A.M., Mason C.C., McKay M.P. and Stockli D.F. (2018). Late Pleistocene glacial transitions in North America altered major river drainages, as revealed by deep-sea sediment. Scientific reports, 8(1), 1-8. DOI:10.1038/s41598-018-32268-7.

Fryirs K.A., Wheaton J.M. and Brierley G.J. (2016). An approach for measuring confinement and assessing the influence of valley setting on river forms and processes. Earth Surface Processes and Landforms, 41(5), 701-710, DOI: 10.1002/esp.3893.

Fryirs K.A. and Brierley G.J. (2012). Geomorphic analysis of river systems: an approach to reading the landscape. John Wiley & Sons.

Fryirs K.A. and Brierley G.J. (2010). Antecedent controls on river character and behaviour in partly confined valley settings: Upper Hunter catchment, NSW, Australia. Geomorphology, 117(1-2), 106-120, DOI: 10.1016/j.geomorph.2009.11.015.

Grill G., Lehner B., Lumsdon A. E., MacDonald G.K., Zarfl C. and Reidy Liermann C. (2015). An index-based framework for assessing patterns and trends in river fragmentation and flow regulation by global dams at multiple scales. Environ. Res. Lett., 10(1), 015001, DOI: 10.1088/1748-9326/10/1/015001.

Grill G., Lehner B., Thieme M. et al. (2019). Mapping the world's free-flowing rivers. Nature, 569, 215–221, DOI: 10.1038/s41586-019-1111-9.

Hais M., Komprdová K., Ermakov N. and Chytrý M. (2015). Modelling the Last Glacial Maximum environments for a refugium of Pleistocene biota in the Russian Altai Mountains, Siberia. Palaeogeography, Palaeoclimatology, Palaeoecology, 438, 135-145, DOI: 10.1016/j.palaeo.2015.07.037.

Hauer C., Skrame K. and Fuhrmann M. (2021). Hydromorphological assessment of the Vjosa river at the catchment scale linking glacial history and fluvial processes. Catena, 207, 105598, DOI: 10.1016/j.catena.2021.105598.

Hauer C. and Pulg U. (2021). Buried and forgotten—The non-fluvial characteristics of postglacial rivers. River Research and Applications, 37(2), 123-127, DOI: 10.1002/rra.3596.

Hauer C. and Pulg U. (2018). The non-fluvial nature of Western Norwegian rivers and the implications for channel patterns and sediment composition. Catena, 171, 83-98, DOI: 10.1016/j.catena.2018.06.025.

He F., Zarfl C., Bremerich V., David J.N., Hogan Z., Kalinkat G., Tockner K., and Jähnig S.C. (2019). The global decline of freshwater megafauna. Global Change Biology, 25(11), 3883-3892, DOI: 10.1111/gcb.14753.

He F., Bremerich V., Zarfl C., et al. (2018). Freshwater megafauna diversity: Patterns, status and threats. Diversity and Distribution; 24, 1395–1404. DOI:10.1111/ddi.12780.

Hedding D.W., Erofeev A.A., Hansen C.D., Khon A.V. and Abbasov Z.R. (2020). Geomorphological processes and landforms of glacier forelands in the upper Aktru River basin (Gornyi Altai), Russia: evidence for rapid recent retreat and paraglacial adjustment. Journal of Mountain Science, 17(4), 824-837.

Hemmelder S., Marra W., Markies H. and De Jong S.M. (2018). Monitoring river morphology & bank erosion using UAV imagery–A case study of the river Buëch, Hautes-Alpes, France. International Journal of Applied Earth Observation and Geoinformation, 73, 428-437, DOI: 10.1016/j.jag.2018.07.016.

Herget J., Agatova A.R., Carling P.A. and Nepop R.K. (2020). Altai megafloods—The temporal context. Earth-Science Reviews, 200, 102995, DOI: 10.1016/j.earscirev.2019.102995.

Hey R.D. (2006). Fluvial Geomorphological Methodology for Natural Stable Channel Design. JAWRA Journal of the American Water Resources Association, 42(2), 357-386.

Huang W., Yang X., Jobe J.A.T., Li S., Yang H. and Zhang L. (2019). Alluvial plains formation in response to 100-ka glacial–interglacial cycles since the Middle Pleistocene in the southern Tian Shan, NW China. Geomorphology, 341, 86-101, DOI: 10.1016/j.geomorph.2019.05.013.

Ibisate A., Ollero A. and Díaz Bea E. (2011). Influence of catchment processes on fluvial morphology and river habitats. Limnetica, 30(2), 0169-182.

Klubnikin K., Annett C., Cherkasova M., Shishin M. and Fotieva I. (2000). The sacred and the scientific: traditional ecological knowledge in Siberian river conservation. Ecological Applications, 10(5), 1296-1306.

Kujanová K. and Matouškova M. (2017). Identification of Hydromorphological Reference Sites Using the New REFCON Method, with and Application to Rivers in the Czech Republic. Ecohgydrology & Hydrobiology, 17, 235-245, DOI: 10.1016/j.ecohyd.2017.06.002.

Langat P.K., Kumar L. and Koech R. (2019). Monitoring river channel dynamics using remote sensing and GIS techniques. Geomorphology, 325, 92-102, DOI: 10.1016/j.geomorph.2018.10.007.

Lehmkuhl F., Klinge M. and Stauch G. (2004). The extent of Late Pleistocene glaciations in the Altai and Khangai Mountains. Developments in Quaternary Sciences, 2, 243-254.

Lemm J.U., Venohr M., Globevnik L., et al. (2021). Multiple stressors determine river ecological status at the European scale: Towards an integrated understanding of river status deterioration. Global Change Biology, 27, 1962-1975, DOI: 10.1111/gcb.15504.

Liu S., Xie Z., Liu B., Wang Y., Gao J., Zeng Y., Xie J., Xie Z., Jia B., Qin P. and Li R. (2020). Global river water warming due to climate change and anthropogenic heat emission. Global and Planetary Change, 193, 103289, DOI: 10.1016/j.gloplacha.2020.103289.

Mackin J.H. (1948). Concept of the graded river, Geol. Soc. Am. Bull., 59, 463-512. (as cited by Rice and Church 2001)

Mahala A. (2020). The significance of morphometric analysis to understand the hydrological and morphological characteristics in two different morpho-climatic settings. Applied Water Science, 10(1), 1-16, DOI: 10.1007/s13201-019-1118-2.

Malatesta L.C. and Avouac J.P. (2018). Contrasting river incision in north and south Tian Shan piedmonts due to variable glacial imprint in mountain valleys. Geology, 46(7), 659-662, DOI: 10.1130/G40320.1.

Malmqvist B. and Rundle S. (2002). Threats to the running water ecosystems of the world. Environmental conservation, 29(2), 134-153, DOI:10.1017/S0376892902000097.

Mueller J. E. (1968). An Introduction to the Hydraulic and Topographic Sinuosity Indexes. Annals of the Association of American Geographers, 58(2), 371-385.

Muhar S. (1996). Habitat improvement of Austrian rivers with regard to different scales. Regulated Rivers Research & Management, 12, 471-482.

Nanson G.C. and Huang H.Q. (2018). A philosophy of rivers: Equilibrium states, channel evolution, teleomatic change and least action principle. Geomorphology, 302, 3-19.

Narozhniy Y. and Zemtsov V. (2011). Current state of the Altai glaciers (Russia) and trends over the period of instrumental observations 1952–2008. Ambio, 40(6), 575-588, DOI: 10.1007/s13280-011-0166-0.

Newbold J. D., O'neill R. V., Elwood J. W. and Van Winkle W. (1982). Nutrient spiralling in streams: implications for nutrient limitation and invertebrate activity. The American Naturalist, 120(5), 628-652.

Newson M. D. and Large A. R. G. (2006). 'Natural' Rivers, 'Hydromorphological Quality' and River Restoration: A Challenging New Agenda for Applied Fluvial Geomorphology. Earth Surface Processes and Landforms, 31, 1606-1624, DOI: 10.1002/esp.1430.

Piégay H., Arnaud F., Belletti B., Bertrand M., Bizzi S., Carbonneau P., Dufour S., Liébault F., Ruiz-Villanueva V. and Slater L. (2020). Remotely sensed rivers in the Anthropocene: State of the art and prospects. Earth Surface Processes and Landforms, 45(1), 157-188, DOI: 10.1016/j.geomorph.2015.05.010.

Rinaldi M., Gurnell A.M., Del Tánago M.G., Bussettini M. and Hendriks D. (2016). Classification of river morphology and hydrology to support management and restoration. Aquatic sciences, 78(1), 17-33, DOI: 10.1007/s00027-015-0438-z.

Rinaldi M., Surian, N. Comiti F. and Bussettini M. (2015). A methodological framework for hydromorphological assessment, analysis and monitoring (IDRAIM) aimed at promoting integrated river management. Geomorphology, 251, 122-136, DOI: 10.1016/j.geomorph.2015.05.010.

Rudoy A.N., (2002). Glacier-dammed lakes and geological work of glacial superfloods in the Late Pleistocene, Southern Siberia, Altai Mountains. Quaternary International, 87(1), 119-140.

Rudoy A.N. and Baker V.R. (1993). Sedimentary effects of cataclysmic late Pleistocene glacial outburst flooding, Altay Mountains, Siberia. Sedimentary Geology, 85(1-4), 53-62, DOI: 10.1016/0037-0738(93)90075-G.

Sala O. E., Stuart Chapin III F., Armesto J. J., Berlow E., Bloomfield J., Dirzo R., Huber-Sanwald E., Huenneke L. F., Jackson R. B., Kinzig A., Leemans R., Lodge D. M., Mooney H. A., Oesterheld M., Poff N. L., Sykes M. T., Walker B. H., Walker M., and Wall D. H. (2000). Global biodiversity scenarios for the year 2100. Science, 287(5459), 1770-1774, DOI: 10.1126/science.287.5459.1770.

Schletterer M., Shevchenko A.A., Yanygina L.V., Manakov Y.A., Reisenbüchler M. and Rutschmann P. (2021). Eindrücke vom Oberlauf des Obs in Russland. Wasserwirtschaft, 111(9-10), 77-85, DOI: 10.1007/s35147-021-0903-7.

Scorpio V., Andreoli A', Zaramella M., Moritsch S., Theule J., Dell'Agnese A., Muhar S., Borga M., Bertoldi W. and Comiti, F. (2020). Restoring a glacier-fed river: Past and present morphodynamics of a degraded channel in the Italian Alps. Earth Surface Processes and Landforms, 45(12), 2804-2823, DOI: 10.1002/esp.4931.

Shahrood A.J., Menberu M.W., Darabi H., Rahmati O., Rossi P.M., Kløve B. and Haghighi A.T. (2020). RiMARS: An automated river morphodynamics analysis method based on remote sensing multispectral datasets. Science of the Total Environment, 719, 137336, DOI: 10.1016/j.scitotenv.2020.137336.

Sokołowski R.J., Molodkov A., Hrynowiecka A., Woronko B. and Zieliński P. (2021). The role of an ice-sheet, glacioisostatic movements and climate in the transformation of Middle Pleistocene depositional systems: a case study from the Reda site, northern Poland. Geografiska Annaler: Series A, Physical Geography, 103:3, 223-258, DOI: 10.1080/04353676.2021.1926241.

Stepinski T. F. and Stepinski A. P. (2005). Morphology of drainage basins as an indicator of climate on early Mars, Journal of Geophysical Research, 110, E12S12, DOI:10.1029/2005JE002448.

Stoddard J.L., Larsen D.P., Hawkins C.P., Johnson R.K. and Norris, R.H. (2006). Setting expectations for the ecological condition of streams: the concept of reference condition. Ecological applications, 16(4), 1267-1276, DOI: 10.1890/1051-0761(2006)016[1267:SEFTEC]2.0.CO;2.

Surazakov A.B., Aizen V.B., Aizen E.M. and Nikitin S.A. (2007). Glacier changes in the Siberian Altai Mountains, Ob river basin (1952–2006) estimated with high resolution imagery. Environmental Research Letters, 2(4), 045017, DOI: 10.1088/1748-9326/2/4/045017.

Surface water resources of the USSR. [Resursy poverkhnostnykh vod SSSR.]. (1962). Vol. 6 Leningrad, "Gidrometeoizdat" [Hydrometeorological Publishing House]: 975 (In Russian)

Tickner D., Opperman J.J., Abell R., Acreman M., Arthington A.H., Bunn S.E., Cooke S.J., Dalton J., Darwall W., Edwards G. and Harrison I., (2020). Bending the curve of global freshwater biodiversity loss: an emergency recovery plan. BioScience, 70(4), 330-342, DOI: 10.1093/biosci/biaa002.

Tímar G. (2003). Controls on Channel Sinuosity Changes: A Case Study of the Tisza River, the Great Hungarian Plain. Quaternary Science Reviews, 22, 2199-2207, DOI: 10.1016/S0277-3791(03)00145-8.

Tomsett C. and Leyland J. (2019). Remote sensing of river corridors: A review of current trends and future directions. River Research and Applications, 35(7), 779-803, DOI: 10.1002/rra.3479.

Torgersen C.E., Le Pichon C., Fullerton A.H., Dugdale S.J., Duda J.J., Giovannini F., Tales É., Belliard J., Branco P., Bergeron N. E., Roy M.L., Tonolla D., Lamouroux N., Capra H. and Baxter C. V. (2022). Riverscape approaches in practice: Perspectives and applications. Biological Reviews, 97(2), 481-504, DOI: 10.1111/brv.12810.

USGS (2019). How Much Water is There on Earth? Available at: https://www.usgs.gov/special-topics/water-science-school/science/how-much-water-there-earth#:~:text=About%2071%20percent%20of%20the,percent%20of%20all%20Earth' s%20water. (Accessed: 21 November 2022).

Volkov I.V., Zemtsov V.A., Erofeev A.A., Babenko A.S., Volkova A.I. and Callaghan T.V. (2021). The dynamic land-cover of the Altai Mountains: Perspectives based on past and current environmental and biodiversity changes. Ambio, 50, 1991-2008, DOI: 10.1007/s13280-021-01605-y.

Wolman M.G. (1954). A Method of Sampling Coarse River-Bed Material. Transactions, American Geophysical Union, 35(6), 951-956.

Vandenberghe J., Kasse C., Popov D., Markovic S.B., Vandenberghe D., Bohncke S. and Gabris G. (2018). Specifying the external impact on fluvial lowland evolution: The last glacial Tisza (Tisa) catchment in Hungary and Serbia. Quaternary, 1(2), 14, DOI: 10.3390/quat1020014.

Vannote R.L., Minshall G.W., Cummins K.W., Sedell J.R. and Cushing C.E. (1980). The river continuum concept. Canadian journal of fisheries and aquatic sciences, 37(1), 130-137.

Ward J.V. (1989). The four-dimensional nature of lotic ecosystems. Journal of the North American Benthological Society, 8(1), 2-8.

Williams H.B. and Koppes M.N. (2019). A comparison of glacial and paraglacial denudation responses to rapid glacial retreat. Annals of Glaciology, 60(80), 151-164, DOI: 10.1017/aog.2020.1.

Woolderink H.A.G., Cohen K.M., Kasse C., Kleinhans M.G. and Van Balen R.T. (2021). Patterns in river channel sinuosity of the Meuse, Roer and Rhine rivers in the Lower Rhine Embayment rift-system, are they tectonically forced? Geomorphology, 375, 107550, DOI: 10.1016/j.geomorph.2020.107550.

Yue S., Ouarda T.B.M.J., Bob´ee B., Legendre P. and Bruneau P. (1999). The Gumbel mixed model for flood frequency analysis. J. Hydrol., 226(1-2), 88-100, DOI: 10.1016/S0022-1694(99)00168-7.

Zarfl C., Berlekamp J., He F., Jähnig S.C., Darwall W. and Tockner K. (2019). Future large hydropower dams impact global freshwater megafauna. Scientific reports, 9(1), 1-10, DOI: 10.1038/s41598-019-54980-8.

Zolnikov I.D., Deev E.V., Kotler S.A., Rusanov G.G. and Nazarov D.V. (2016). New results of OSL dating of Quaternary sediments in the Upper Katun'valley (Gorny Altai) and adjacent area. Russian Geology and Geophysics, 57(6), 933-943, DOI: 10.1016/j.rgg.2015.09.022.

Zolnikov I.D., Deev E.V., Nazarov D.V. and Kotler S.A. (2015). Comparative analysis of megaflood deposits and alluvium of the Chuya and Katun'river valleys (Gorny Altai). Russian Geology and Geophysics, 56(8), 1162-1172, DOI: 10.1016/j.rgg.2015.07.007.

APPENDIX

Table A.1. Summary of the observed morphological parameters along the Biya. Landscape reading elements: Active channel width (AC), active floodplain width (AF), and morphological floodplain width (MF), and sinuosity: Standard (SSI), hydraulic (HSI), and topographic (TSI) sinuosity index

	Section	River Kilometer		Elevation			Slope	AC			AF			MF			Sinuosity			
	Nr.	Start	End	Min.	Max.	Avg.	Avg.	Min.	Max.	Avg.	Min.	Max.	Avg.	Min.	Max.	Avg.	SSI	HSI	TSI	
	[-]	[km]	[km]	[m a.s.l.]			[‰]	[m]			[m]			[m]			[-]	[%]		
upper Biya	1	0	10	420	442	429	-1.19	50	805	384	239	461	335	489	937	630	1.1128	51.98	48.02	upper Biya
	2	10	20	406	432	415	-2.12	45	190	112	241	783	467	445	1453	990	1.1515	56.65	43.35	
	3	20	30	389	417	399	-0.40	42	139	87	226	762	447	809	1297	1032	1.1749	64.74	35.26	
	4	30	40	360	393	382	-1.20	71	163	115	166	506	365	1221	3898	2740	1.3232	65.09	34.91	
	5	40	50	357	381	370	-3.38	65	312	149	269	711	479	2159	2928	2410	1.2603	81.16	18.84	
	6	50	60	333	347	339	-1.52	148	324	232	194	470	310	1211	2363	1920	1.0005	6.40	93.60	
	7	60	70	320	332	327	-1.40	221	503	297	189	598	302	1586	3971	2936	1.5492	92.86	7.14	
	8	70	80	305	318	311	-1.40	180	658	366	212	482	359	1713	3573	2201	1.0634	30.00	70.00	
	9	80	90	290	304	297	-1.60	360	1148	747	275	694	463	1346	2346	1767	1.2153	57.38	42.62	
middle Biya	10	90	100	278	288	283	-1.20	90	595	207	180	735	412	907	2507	1702	1.2355	82.56	17.44	middle Biya
	11	100	110	268	276	272	-1.00	69	197	145	390	904	552	2275	2801	2555	1.0173	19.95	80.05	
	12	110	120	257	266	261	-1.10	106	210	146	255	1285	731	1698	4211	2948	1.0516	60.30	39.70	
	13	120	130	247	255	251	-0.80	87	311	193	338	1840	955	2198	4184	3078	1.1731	65.92	34.08	
	14	130	140	237	247	242	-1.00	133	450	251	230	2126	1088	3616	4577	4007	1.0949	81.56	18.44	
	15	140	150	226	237	232	-1.10	173	337	246	535	4125	1713	4743	6847	5913	1.1579	88.03	11.97	
	16	150	160	220	226	223	-0.70	164	971	301	478	1752	1153	6508	7419	6941	1.5480	97.91	2.09	
	17	160	170	201	232	216	-0.60	186	938	371	429	1882	1039	4590	7979	6594	1.5325	62.74	37.26	
	18	170	180	208	213	211	-0.70	187	708	303	331	1310	828	392	2914	1579	1.0577	51.93	48.07	
	19	180	190	202	206	203	-0.40	199	690	325	502	1783	904	502	1944	1099	1.1183	42.30	57.70	
	20	190	200	197	202	199	-0.50	64	554	225	1265	2133	1661	1965	3326	2899	1.0268	28.95	71.05	
lower Biya	21	200	210	190	207	195	-0.38	72	272	142	630	4205	2135	3036	4163	3555	1.0048	4.19	95.81	lower Biya
	22	210	220	185	193	188	-0.92	73	223	157	416	2143	1039	4094	8713	6926	1.7374	81.27	18.73	
	23	220	230	177	194	181	-0.73	133	267	168	325	1326	646	6212	8452	7672	1.1842	88.67	11.33	
	24	230	240	170	178	174	-0.74	133	395	219	763	2388	1321	4704	5999	5511	1.2423	90.71	9.29	
	25	240	250	165	170	167	-0.44	98	636	224	426	1834	1142	3049	4195	3415	1.1464	95.77	4.23	
	26	250	260	163	165	164	-0.20	146	672	234	300	1186	673	3233	3869	3448	1.2488	94.40	5.60	
	27	260	270	162	163	162	-0.22	137	1008	493	280	1352	658	3115	3912	3595	1.2914	83.06	16.94	
	28	270	280	160	161	160	-0.08	239	841	450	432	1596	1020	2517	3763	2966	1.2847	94.97	5.03	
	29	280	290	160	164	160	0.00	156	1538	505	443	1627	768	2158	3178	2686	1.0200	38.68	61.32	
	30	290	300	160	160	160	0.00	182	562	278	317	1695	789	2517	4591	3718	1.1279	53.44	46.56	

Table A.2. Summary of the observed morphological parameters along the Biya based on 10 km stretches. Verbal and qualitative description (for category definitions cat.A to F see below)´

	Section	River Kilometer		Topographic Structures	Channel		Valley Slopes (orogr. side)		Valley Orientation			Valley Width			
	Nr.	Start	End	Prominent Elements	Type	Width	left	right	current	previous	following	current	previous	following	
	[-]	[km]	[km]	[-]	[cat.A]	[cat.B]	[cat.C]		section [cat.D]			section [cat.E/F]			
upper Biya	1	0	10	Outflow Lake Teletskoye, narrow valley cross sections	3	2	1	1	2		2	1		1	upper Biya
	2	10	20		2	2	2	2/1	2	2	2	2	3	2	
	3	20	30	Valley incision/ topographic constraints that force the valley to bend to the orogr. Right	2	1	2	1/3	2	2	3	1	2	1	
	4	30	40	valley incision followed by significant widening	1	1	2	2	3	2	1	2	3	3	
	5	40	50		2	2	2	2	1	3	1	1	1	3	
	6	50	60	Valley incision at rkm 58/59	1	2	3	3	1	1	2	1	1	1	
	7	60	70	Significant widening	2	2	1	1	2	1	3	2	3	3	
	8	70	80		2	3	2	2	3	2	1/4	2	1	3	
	9	80	90	tributary (orogr. Right) in close vicinity over most part	2	2	1	3	1/4	3	1	2	1	2	
middle Biya	10	90	100	more complex island structure between rkm 94-97	2	2	2	3	1	1/4	2	2	2	1	middle Biya
	11	100	110	more complex island structure around rkm 110	3	3	2	3	2	1	2	1	3	1	
	12	110	120	more complex island structure around rkm 110 and rkm 119	3	3	3	1	2	2	1	2	3	2	
	13	120	130	rkm 120-126	4	2	2	2	1	2	1	2	2	1	
	14	130	140		5	2	2/1	2	1	1	1	1	3	1	
	15	140	150	superordinate valley bend to the orogr. leftbetween rkm 140-175	5	3	3	3	1	1	1	2	3	1	
	16	150	160	superordinate valley bend to the orogr. leftbetween rkm 140-175	4	3	3	3	1	1	3	1	3	3	

middle Biya	17	160	170	superordinate valley bend to the orogr. leftbetween rkm 140-175	5	3	3	2	3	1	2	2	1	3	middle Biya
	18	170	180	superordinate valley bend to the orogr. leftbetween rkm 140-175 followed by superordinate valley bend to the orographic right between rkm 175-190	5	3	2	2	2	3	4/2	2	1	3	
	19	180	190	superordinate valley bend to the orographic right between rkm 175-190, distinctive bend to the left (rkm 180-184) upstream of hill structure	2	2	1	2	4/2	2	3	2	1	1	
	20	190	200	superordinate valley bend to the orogr. Left between rkm 190-210	4	3	1	2	3	4/2	3	2	3	1	
lower Biya	21	200	210	superordinate valley bend to the orogr. Left between rkm 190-210	2	2	1	3	3	3	1	2	3	1	lower Biya
	22	210	220	Significant widening, bend near rkm 220 initiatend by hill structure	2	2	2/1	2	1	3	1	2	3	1	
	23	220	230		2	2	1/2	3	1	1	1	2	3	3	
	24	230	240		2	3	3	3	1	1	1	2	1	3	
	25	240	250		5	3	2	2	1	1	1	1	1	2	
	26	250	260	clear signs of human infrastructure	1	2	2	2	1	1	1	1	2	2	
	27	260	270	clear signs of human infrastructure	2	3	2	2	1	1	1	1	2	2	
	28	270	280	clear signs of human infrastructure	2	3	2	2	1	1	2	1	2		
	29	280	290	clear signs of human infrastructure, valley borders hard to define	5	3	2	2	2	1	2				
	30	290	300	clear signs of human infrastructure, valley borders hard to define, orogr. Left interactions with Katun	2	3	3	2	2	2					

[A]Channel Type	1	one main channel, hardly any developed Islands
	2	1 to 3 developed islands, subordinate sidearms
	3	one well developed Island about every 1 km
	4	more than one (main) channel for more than half of the length
	5	complex, several side arms for (almost) the whole length
[B]Channel Width	1	rather constant channel width
	2	slight channel width variations
	3	strong channel width variations
[C]Valley Slopes	1	steep
	2	flat
	3	flat, dominated by tributary confluence
[D]Valley Orientation	1	straight/unidirectional
	2	sinusoidal
	3	meander bend to the orographic left
	4	meander bend to the orographic right
[E]Valley width	1	rather constant valley width
	2	noticeable valley width variations
[F]Valley Width in Context	1	narrower than previous section
	2	comparable width to previous section
	3	wider than previous section

Table A.3. Summary of the observed morphological parameters along the Biya based on 10 km stretches. Hydrological Information

	Section	River Kilometer		Tributaries*				Discharge (Q)**		
	Nr.	Start	End	Name(s)	orographic side(s)	Catchment Size	Length	Gauging Station	Q_{mean}	
	[-]	[km]	[km]	[-]	[-]	[km^2]	[km]	[-]	[m^3s^{-1}]	
upper Biya	1	0	10	Yurtok	right	?	17	Artybash	226.75	upper Biya
	2	10	20	Pyzha	left	1180	103			
	3	20	30	Kebezenka - Sarakoksha	right - left	? - 3150	16 - 90			
	4	30	40					Kebezen	246.86	
	5	40	50	Tula - stream without name	right - right	384 - ?	54 - 10			
	6	50	60	Bava	left	?	25			
	7	60	70	Tandoshka	right	209	42			
	8	70	80							
	9	80	90	Lebed'	right	4500	175	Turochak	323.83	
middle Biya	10	90	100	Alemchir - Polysh	right - left	? - ?	10 - 13			middle Biya
	11	100	110	Ulmen	right	?	48			
	12	110	120	Ushpa	right	214	24			
	13	120	130	Tibezya	left	?	39			
	14	130	140	Bol. Kuyut - Balyksa	right - left	223 - ?	33 - 31			
	15	140	150	Uchurga	right	?	24			
	16	150	160							
	17	160	170	Kutenek	left	?	14			
	18	170	180	Kozha	left	4210	63			
	19	180	190	Chapshushka	left	?	22			
	20	190	200							
lower Biya	21	200	210	Nenya	right	2210	185			lower Biya
	22	210	220	Souskanikha	left	?	17			
	23	220	230							
	24	230	240	Talitsa - Bekhtemir	left - right	? - 665	28 - 117			
	25	240	250							
	26	250	260							
	27	260	270							
	28	270	280							
	29	280	290					Biysk	476.36	
	30	290	300							

*Information from Russian Water Register: http://textual.ru/gvr/index.php?card=187196
**Data from Russia ArcticNET (Point IDs XXX as in body of text above):
https://www.r-arcticnet.sr.unh.edu/v4.0/ViewPoint.pl?View=ALL&Unit=ms&Point=XXXX